

# On the size of knots in ring polymers.

B. Marcone,<sup>1</sup> E. Orlandini,<sup>2,3</sup> A. L. Stella,<sup>2,3</sup> and F. Zonta<sup>1</sup>

<sup>1</sup>*Dipartimento di Fisica, Università di Padova, I-35131 Padova, Italy.*

<sup>2</sup>*Dipartimento di Fisica and Sezione CNR-INFN,  
Università di Padova, I-35131 Padova, Italy.*

<sup>3</sup>*Sezione INFN, Università di Padova, I-35131 Padova, Italy.*

## Abstract

We give two different, statistically consistent definitions of the length  $\ell$  of a prime knot tied into a polymer ring. In the good solvent regime the polymer is modelled by a self avoiding polygon of  $N$  steps on cubic lattice and  $\ell$  is the number of steps over which the knot “spreads” in a given configuration. An analysis of extensive Monte Carlo data in equilibrium shows that the probability distribution of  $\ell$  as a function of  $N$  obeys a scaling of the form  $p(\ell, N) \sim \ell^{-c} f(\ell/N^D)$ , with  $c \simeq 1.25$  and  $D \simeq 1$ . Both  $D$  and  $c$  could be independent of knot type. As a consequence, the knot is weakly localized, i.e.  $\langle \ell \rangle \sim N^t$ , with  $t = 2 - c \simeq 0.75$ . For a ring with fixed knot type, weak localization implies the existence of a peculiar characteristic length  $\ell^\nu \sim N^{t\nu}$ . In the scaling  $\sim N^\nu$  ( $\nu \simeq 0.58$ ) of the radius of gyration of the whole ring, this length determines a leading power law correction which is much stronger than that found in the case of unrestricted topology. The existence of such correction is confirmed by an analysis of extensive Monte Carlo data for the radius of gyration. The collapsed regime is studied by introducing in the model sufficiently strong attractive interactions for nearest neighbor sites visited by the self-avoiding polygon. In this regime knot length determinations can be based on the entropic competition between two knotted loops separated by a slip link. These measurements enable us to conclude that each knot is delocalized ( $t \simeq 1$ ).

PACS numbers: 36.20.Ey, 64.60.Ak, 87.15.Aa, 02.10.Kn

## I. INTRODUCTION

Various forms of topological entanglement play a fundamental role in determining equilibrium and dynamical properties of single chain and multi-chain polymeric systems [1, 2], with relevant consequences also for biological matter. For instance, the presence of a knot can be an obstacle to the processes of duplication and segregation of DNA in bacterials [3]. Indeed, there exist topoisomerase enzymes whose function is precisely that of controlling the topology of circular DNA [4, 5]. The knots and links which are ubiquitous in higher molecular multi-chain melts and solutions can profoundly affect properties of such systems like viscosity or resistance to rupture [6]. Knots can even be found in the native state of some proteins [7, 8, 9, 10]. and may play an important role in their stabilization with respect to denaturing agents and in their folding dynamics.

The description of the consequences of topological entanglement in polymer physics poses theoretical and numerical challenges which only relatively recently started to be faced with some success [11] [12]. An interesting issue addressed in the last years is that of establishing whether knots tend to be “spread” over the whole polymer or “localized” within a short portion of the chain (Fig. 1). If properly quantified, the degree of localization of (prime) knots is expected to play an important role in the discussion of both equilibrium and dynamical properties of knotted macromolecules. For example, if the knot is localized to some degree in a long ring, the logarithmic correction to the ring entropy per monomer should drastically change with respect to that of the unknotted case [13]. On the other hand, the knot could behave in such a way that its average “length” grows with the  $t$ -th power ( $0 < t < 1$ ) of the total ring length  $N$ . Corrections to scaling associated to this length should then be expected for the long chain behavior of measurable quantities like the gyration radius [14]. These corrections should be detectable as peculiar of rings with prime knot, but could not be predicted within the framework of approaches like the field theoretical renormalization group, which treats only the case of “phantom” ring polymers with unrestricted topology. The size of the knot in a DNA ring should also strongly affect the action of topoisomerases or the mobility of the ring in gel electrophoresis experiments [15]. Furthermore, recent experiments of DNA micromanipulation by optical tweezers have shown that it is possible to tie specific knots into the macromolecule [16] and to observe their motion within a viscous solution [17]. For this problem the knowledge of the length of

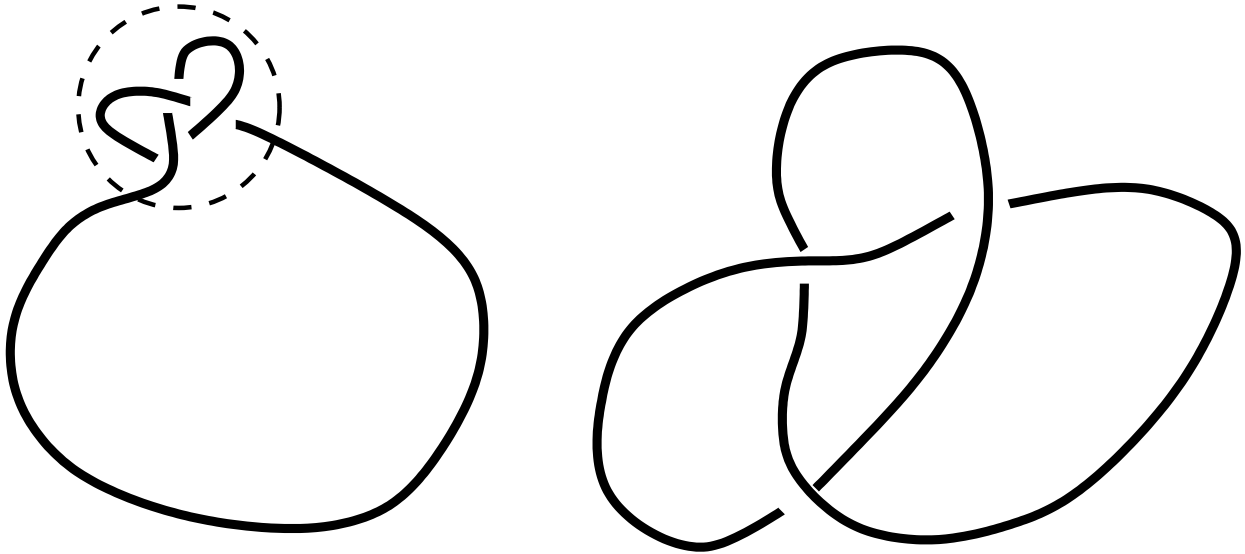


FIG. 1: On the left we see a tight knot: it is easy to say that the knotted arc is that within the small sphere (dashed circle). On the right the knot is delocalized within the curve.

the entangled region is essential, since it directly affects the knot diffusion coefficient [17].

In spite of some early indications that prime knots in ring polymers in good solvent are likely to be localized in small portions of the chain [13, 18], sufficiently direct and quantitative evidence of this property remained for long a major challenge. This is mainly due to the difficulty of locating the knot of a closed curve in a consistent way. A possible procedure is that of isolating a trial open portion of the curve and of checking whether the new ring obtained by joining its extremes with a topologically “neutral” closure still contains the original knot, or not. The knot length should then be identified with that of the smallest portion for which the knot remains. Such procedure relies on the notion of knotted arc that is not well defined mathematically [19]. Indeed, since knots are embeddings of *circles* [20], in a strict mathematical sense no open string can be knotted: continuous transformations acting on such string can always bring it into an untangled shape. For a general closed curve knottedness is a global property: we can not state that a portion is knotted, but only that the whole curve is (Fig. 2). Nevertheless, as we show here, when dealing with a whole sample of closed curve configurations the notion of knot length may acquire a physical meaning, at least in a statistical sense.

A definition of knot length may be much more easy to give for flat knots [21], i.e. knots in ring polymers that are confined in two dimensions [22]. Physical examples include polymer

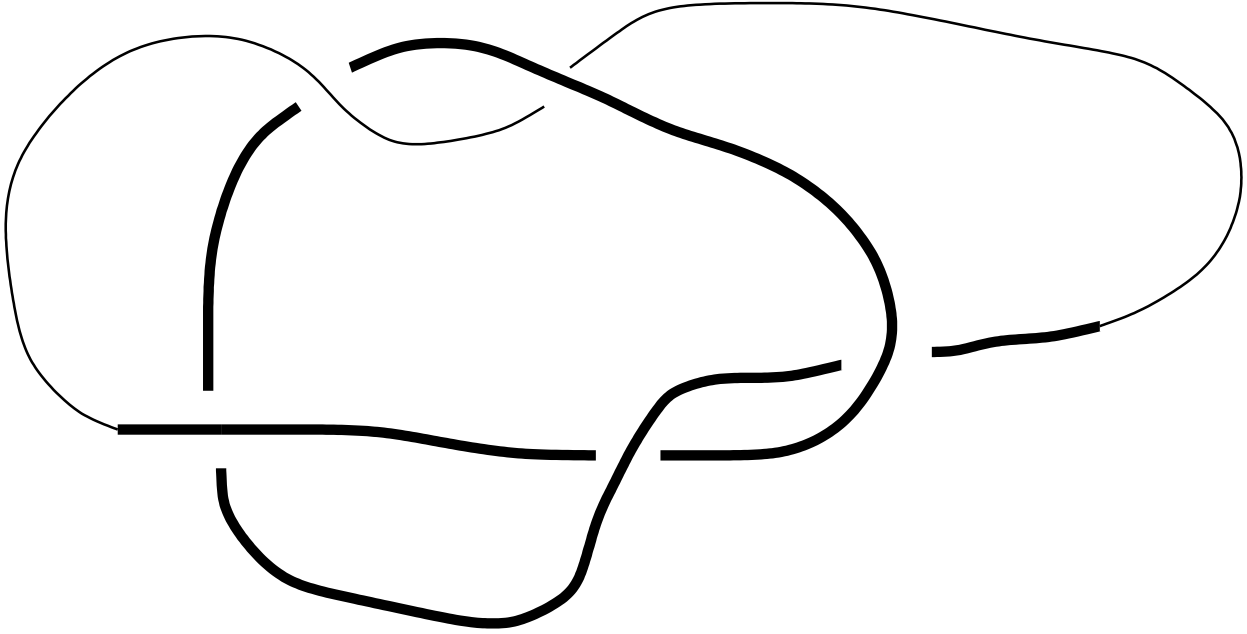


FIG. 2: The thicker arc, once extracted from the rest of the curve, seems to be knotted while the whole curve is not.

rings adsorbed on a plane by adhesive forces [23] or macroscopic necklaces flattened under gravity onto a vibrating plane [24]. The configurations of such adsorbed rings would be similar to the planar projections used in knot theory to compute topological invariants and classify knots [20]. Under the simplifying assumption that the number of overlaps is restricted to the minimum compatible with its topology (for example 3 for the trefoil knot), the length of the hosted flat knot can be unambiguously defined and its statistical behavior, as a function of the number of monomers of the ring, can be studied analytically [22] and numerically [25]. In the good solvent regime flat knots were found to be strongly localized. This approach has also been extended to polymer rings that undergo collapse from the swollen (high temperature) to the compact (low temperature) regime and it was found that globular flat knots are delocalized ( $t \simeq 1$ ) [25, 26, 27]. However, the results on localization and delocalization of flat knots apply to a model which is a too crude representation of knots in three dimensions, which are the challenge here.

In a recent Letter [14] we reported a preliminary investigation of the size of knots in a flexible polymer ring fluctuating in equilibrium in 3D. By modelling the ring configurations as self-avoiding polygons (SAPs) on a cubic lattice, we could take fully into account excluded volume. Thanks to the inclusion of short range attractive interactions, upon lowering the

temperature  $T$ , the polymer ring did undergo a collapse transition from a coil to a globule shape at the  $\theta$  point temperature [28].

To measure the average size of the knots in the high temperature swollen regime, we followed two different methods [14]. The first one was based on the cutting-closing strategy already outlined above. In order to test the consistency of the results we also adopted a completely new strategy based on the entropic competition between two knotted loops into which a ring can be partitioned by a slip link. If each one of the two loops contains, e. g., a prime knot, one expects a dominance of equilibrium configurations in which one of the loops is entropically tightened, while the other one gains almost the whole length of the ring. It is then tempting to identify this form of tightening of the loop with the entropic tightening of the knot it contains. This last tightening could also be the same as that occurring within a singly knotted fluctuating ring.

In Ref. [14] we gave evidence that in the swollen regime prime knots are weakly localized with  $t \sim 0.75$ . This result was obtained with the two independent methods above, by fitting the power law behavior of the average knot length as a function of the total ring length. Similar methods were subsequently applied in Ref. [29] to an off-lattice model of open polyethylene chain, obtaining results for the localization of the trefoil knot in qualitative agreement with ours.

One of the aims of the present work is to address the issue of the consistency of the method of knot localization study based on cutting and closing and that based on entropic competition of loops more systematically, by testing other knot types and, most important, by analyzing more globally the probability distribution functions (PDFs) of the knot length measured in the different cases.

Another purpose of the present work is that of investigating the issue of scaling corrections for ring polymers with fixed topology. Recently, an attempt was made to infer the localization properties of prime knots from the scaling correction detected in the force-extension plots of knotted polymers whose extremes are subjected to a force [30]. However, the results appeared consistent with a power law behavior of the average knot length rather different from those we detected in ref [14] by our direct measurement. Moreover, the correction estimated there appeared weaker than the correction predicted by the field theoretical renormalization group methods for a polymer with unrestricted topology.

A further result, first established in [14] is that below the theta temperature, in the

collapsed phase, knots are delocalized  $t \simeq 1$ . This important conclusion, further supported by results in Ref. [29], calls for a more systematic discussion in view of the relevance of topological entanglement in globular polymers and biopolymers.

The plan of this paper is as follows. In the next section we describe the model and some details of the methods of simulation. The direct measure method will be introduced in Section III and Section IV, where we will discuss also how one can discuss the PDF of the knot length. Section V is dedicated to the knot length evaluation based on the entropic competition between two loops. This second method is the only one safely applicable in the low temperature collapsed regime, and we will present the result obtained for this regime in a further Section (VI). In Section VII, we discuss the implications that the weak localization of knots in good solvent has on the scaling behavior of the mean square radius of gyration of polymer rings and on its corrections. We close in Section VII with a general discussion of the results.

## II. MODEL AND SIMULATION METHODS

We model flexible ring polymers in good solvent by self-avoiding polygons (SAPs) on the cubic lattice, i.e. closed lattice walks whose steps can visit each edge and each vertex of the lattice at most once [28]. Whenever necessary we introduce in our model an attractive interaction potential which lowers the total energy by  $\epsilon > 0$  whenever two nearest-neighbor lattice sites are visited by non-consecutive vertices of the SAP. This attractive interaction is sufficient to induce a theta collapse at sufficiently low temperature  $T$  [28]. The Hamiltonian of a configuration  $\omega$  with  $N_i(\omega)$  nearest neighbor interactions is then  $H(\omega) = -\epsilon N_i(\omega)$ . For a fixed temperature  $T$ , configurations  $\omega(\tau)$ , with a fixed knot type  $\tau$ , are sampled at equilibrium by using a Monte Carlo approach based on the BFACF algorithm, [31] [32]. This is an algorithm which samples along a Markov chain in the configuration space of polygons of variable  $N$  and with fixed knot type. The statistical ensemble considered is thus grand canonical, with a fugacity  $K$  assigned to each polygon step. We adopt this algorithm because it preserves the topology and is irreducible within each set of configuration having the same knot type [33]. At a given  $T$  we used a multiple Markov chain (MMC) procedure [34] in which configurations are exchanged among ensembles having different step fugacities [35]. This is done in order to improve the efficiency of the sampling, especially at low  $T$ . In our

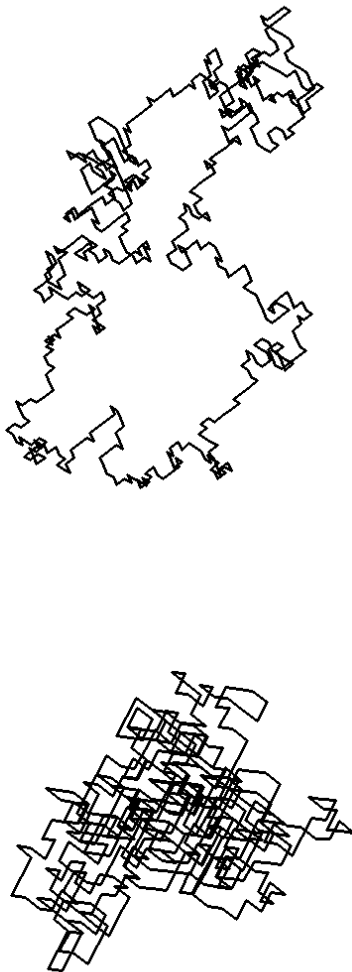


FIG. 3: Two knotted ( $3_1$ ) SAP configurations at equilibrium sampled by a BFACF algorithm: the top configuration refers to the swollen regime while the bottom one to the collapsed phase.

simulations in the swollen regime the MMC's combined up to 10 processes at different  $K$ 's ranging from  $K = 0.2109$  up to  $K = 0.2130$  [36].

A relative disadvantage of the BFACF sampling method is that correlation times are relatively long, making it difficult to collect a sufficient statistics of uncorrelated data at large  $N$ . To improve the statistics for high values of  $N$  in our simulations of knotted SAPs, in the direct measure for the  $3_1$  and the  $4_1$  knots we also made use of a different sampling procedure based on the two-points pivot algorithm [37]. The two-points pivot algorithm is known to

be ergodic in the set of all SAP's with fixed  $N$  and quite efficient in sampling uncorrelated configurations [37]. Unfortunately, pivot moves can change the knot type and a check of the topology of each sampled SAP configuration is needed. This is done by calculating the Alexander polynomial  $\Delta(z)$  in  $z = -1$  and  $z = -2$  [20]. The sampled configurations are then partitioned according to their knot type and the cut and join procedure is performed as before. Note that, since it explores the whole space of  $N$ -step SAPs, the Pivot algorithm is not very efficient in sampling small  $N$  configurations with fixed knot type. For example for  $N = 1000$  the probability of forming a knot is  $\sim 0.004$  [38, 39] meaning that one should wait on average 1000 uncorrelated unknotted configurations before seeing a knotted one. However for  $N > 1000$  simple prime knots start to appear with a sufficient frequency and a reasonable statistics at fixed knot type starts to be possible.

### III. DIRECT MEASURE OF THE KNOT LENGTH: THE CUT AND JOIN PROCEDURE

For each sampled polygon with fixed prime knot type  $\tau$  we measure the length  $\ell$  by determining the shortest possible arc that contains the knot. The idea is rather intuitive and has been considered in previous works on topological entanglements by several authors [14, 18, 19, 40]. The ways in which this method can be implemented can be different and may reveal very important in order to lower systematic errors as we will discuss below. Our procedure works as follow [14]: given a knotted configuration we extract open arcs of different length by following a recursive procedure. Each arc is then converted into a loop by joining its ends at infinity with a suitable path (Figure 4) and the presence of the original knot is checked by computing, on the resulting loop, the Alexander polynomial  $\Delta(z)$  in  $z = -1$  and  $z = -2$  [20, 41]. Clearly, the additional path (dotted in Fig. 4) can topologically interfere with the original arc (despite the procedure tries to avoid this as much as possible) and this could be a source of systematic errors (see Fig. 2). This is a disadvantage common to all the procedures that define a knotted arc by closing it into a loop [18, 19]. Our goal here is to find an optimal closure procedure that minimizes such error. Moreover, as proposed in [14], we expect that the systematic inconsistencies of which this method suffers, should not affect the asymptotic statistical characterization of localized knots.

A rough indication of the systematic error can be given by counting how many times

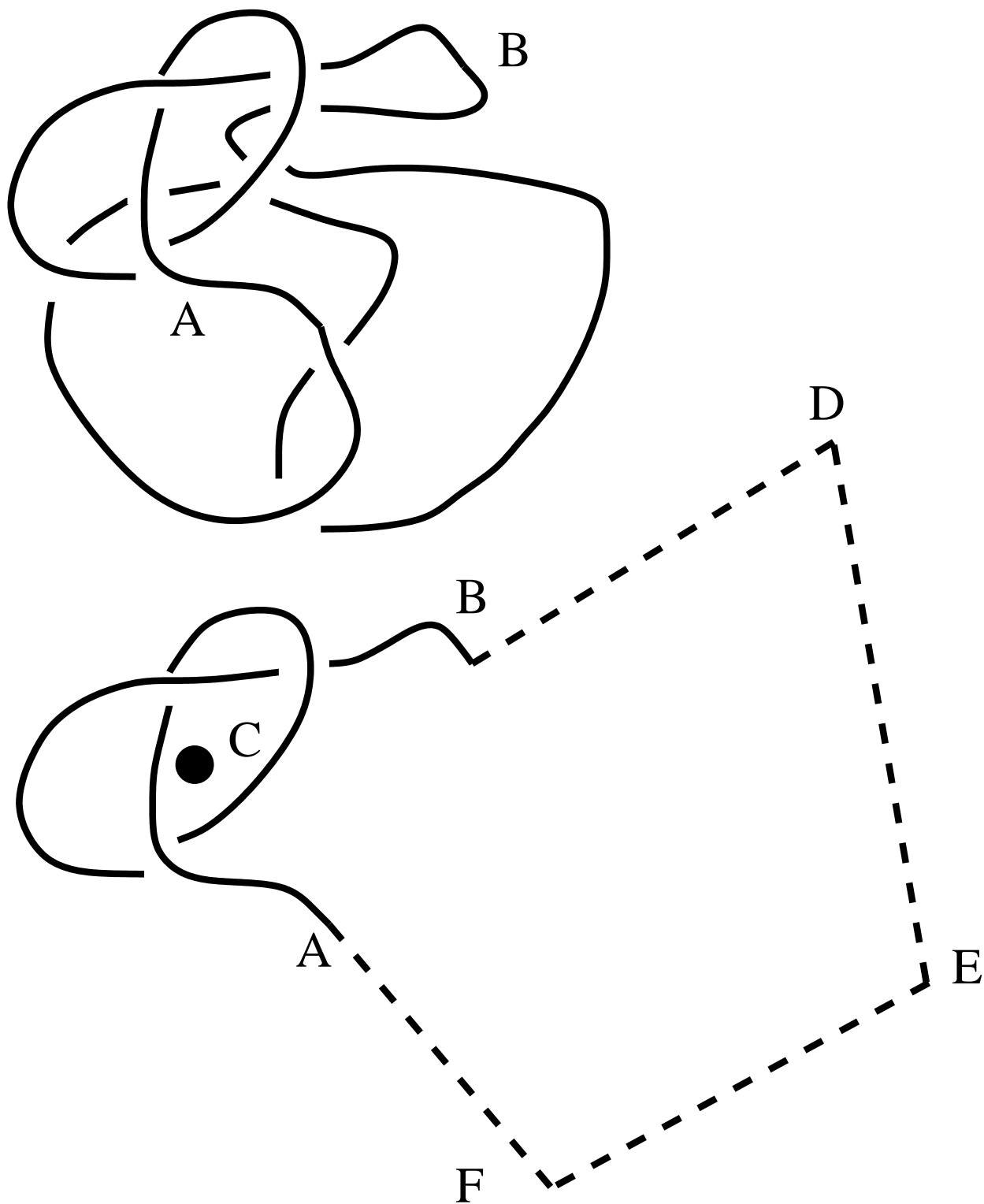


FIG. 4: A sketch of how the closure scheme works: for a given extracted arc with extremes  $A$  and  $B$  we compute the center of mass  $C$  and construct two segments that go far from it (they are constructed on the line connecting  $C$  with  $A$  and  $B$ ). We then complete the loop by connecting the extremes of these segments ( $D$  and  $F$ ) to a point distant from the arc ( $E$ ).

prime knot	$t$
$3_1$	$0.67 \pm 0.05$
$4_1$	$0.77 \pm 0.07$
$5_1$	$0.80 \pm 0.07$
$5_2$	$0.80 \pm 0.05$
$7_1$	$0.85 \pm 0.08$

TABLE I: Estimates of the knot size exponent  $t$  by the cut and join approach. They have been obtained by a linear fit of the log-log plots of Fig. 5. For the  $3_1$  and the  $4_1$  knots the estimates are based on both BFACF and pivot data.

the cut and join procedure finds a knot in arcs extracted from unknotted rings. For our algorithm this test gives a percentage of errors, of the order of 0.2%, with  $N = 500$ , quite low if compared, for example, to the error estimate in [18] for a similar system. A possible explanation is that in [18] the closure is chosen randomly, while in our case it is deterministic and conceived to avoid the pre-existing skein as much as possible.

The procedure we follow in order to identify the shortest arc containing the knot for each SAP configuration, is of iterative type and realizes a progressive reduction of the length of several initial trial arcs.

#### IV. DATA ANALYSIS AND RESULTS

We first focus on the size of prime knots for rings at equilibrium in the high temperature regime. In Ref. [14] we gave preliminary results indicating that in the swollen phase the trefoil and the figure eight knot are weakly localized. Our aim is to make these results more robust by considering other prime knots. Here and in the following, brackets indicate fixed  $N$  averages, obtained, whenever necessary, by a suitable binning of the data. For a fixed knot type we sampled roughly  $10^6$  uncorrelated SAP configurations and for each one of those we estimated the size of the hosted knot by the procedure previously described. In Fig. 5 we show the  $N$  dependence of the average knot size  $\langle \ell \rangle$  obtained in this way for different prime knots. The plots give evidence that  $\langle \ell \rangle \sim N^t$  in all cases. By performing log-log fits of the data and a finite size scaling analysis, we obtain the  $t$  estimates reported in table I. These

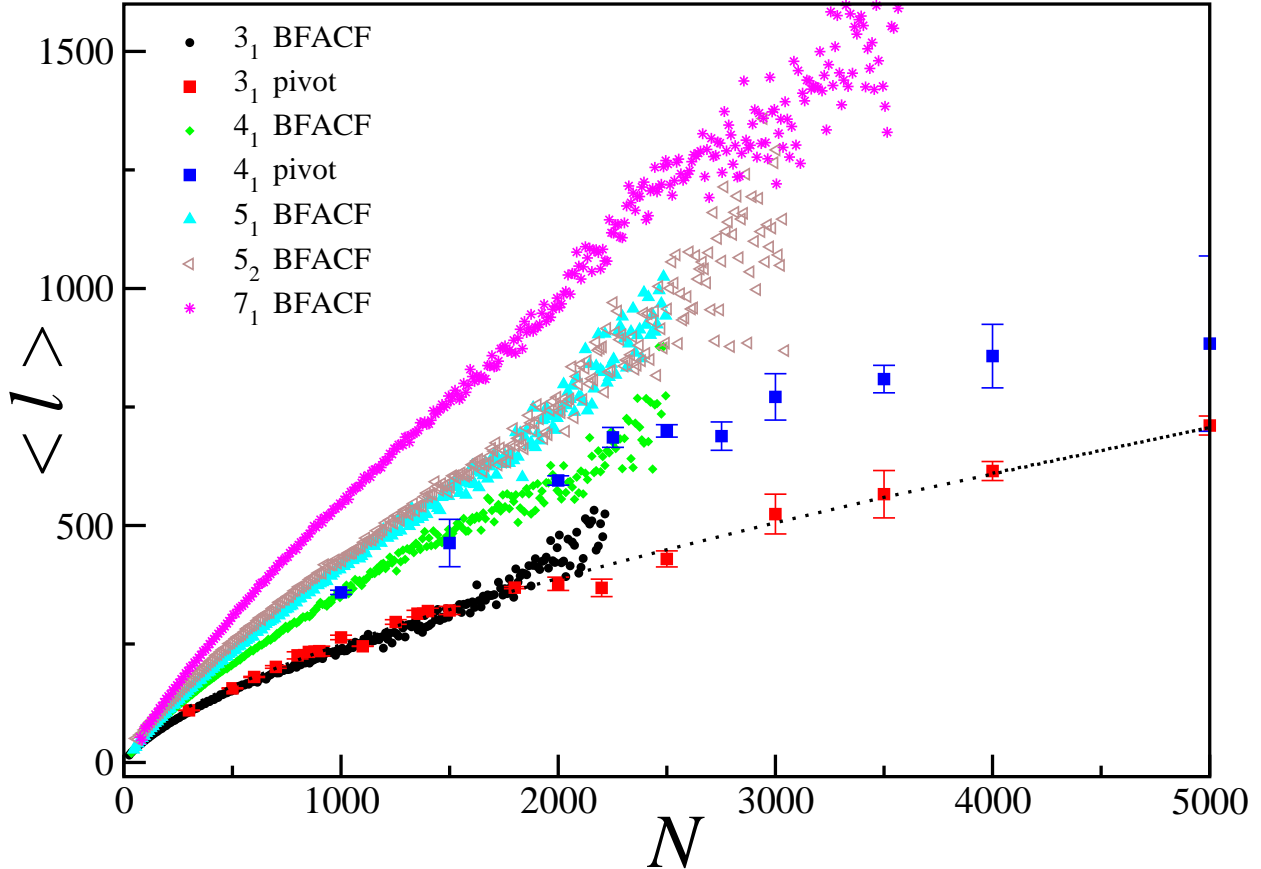


FIG. 5: Average knot size  $\langle \ell \rangle$  as a function of the total length of the polygon  $N$  for different prime knots. Filled symbols correspond to BFACF data, whereas empty symbols represent determinations obtained by the pivot algorithm. The BFACF data has been binned in  $N$ . The dotted curve corresponds to a fit of the form  $\langle \ell \rangle \simeq AN^t$  for the  $3_1$  with  $t$  given by the estimated value in Table I. Note that the data for  $5_1$  and  $5_2$  are almost superimposed.

estimates give a good evidence that prime knots are weakly localized in the swollen regime, i.e.  $t < 1$ . Moreover the overlaps of the plots for  $5_1$  and  $5_2$ , seem to suggest that knots with the same minimal crossing number have very close average size, even for relatively small  $N$ .

The possible dependence of the exponent  $t$  on the knot type is however less clear and to clarify the issue both a better sampling at high  $N$  and a systematic analysis of finite size corrections are needed. From Fig. 5 one can indeed notice that for large  $N$  the BFACF sampling technique starts to deteriorate since the statistics becomes quite poor. This is due to the difficulty of sampling properly the high  $N$  region of the configurational space, since the BFACF algorithm has the disadvantage of very long autocorrelation times [31, 32, 37].

For the knots  $3_1$  and  $4_1$  we complemented our BFACF determinations of  $\langle \ell \rangle$  with data obtained from the two-points pivot algorithm mentioned in Section 2. The average knot lengths obtained with this simulation method overlap the BFCAF estimates in Fig. 5 for  $N \leq 2500$ . The pivot data extend up to  $N \sim 3500$  and are more consistent with the expected power law behavior in the high  $N$  region. One can see a tendency of the exponent to grow with increasing number of the minimal crossing number of the knots. However, the statistical uncertainty is relatively large and it is legitimate to suspect finite size corrections to be stronger for more complex knots.

As far as the scaling analysis is concerned, a more solid and detailed control should be achieved by analyzing the full probability distribution function (PDF) of  $\ell$  as a function of  $N$  i.e.  $p(\ell, N)$ . In analogy with previous works on similar problems [42] [43] one can assume, for the PDF, the following scaling form:

$$p(\ell, N) = N^{-c} f\left(\frac{\ell}{N^D}\right). \quad (1)$$

where the scaling function  $f$  is expected to approach rapidly zero as soon as  $\ell > N^D$ , ( $D \leq 1$ ). The quantity  $N^D$  is a sort of cutoff on the maximum value  $\ell$  can assume. We expect  $D = 1$ , because there are no reason *a priori* to think that there exists some ‘topological cutoff’ which limits the size of the knot. Unfortunately, to look at the scaling behavior of the PDF directly, e.g. by means of collapse plots, is a quite difficult task that needs a huge amount of data and is not feasible in this context. We can instead perform an analysis based on the scaling behavior of the moments of the PDF in Eq. (1) [44]. This method relies on the following consideration: given the scaling behavior (1) for the PDF, its  $q$ -th moment ( $q > 0$ ) should obey the asymptotic law:

$$\langle \ell^q \rangle \sim N^{Dq+D(1-c)} \equiv N^{t(q)} \quad (2)$$

and the two parameters  $D$  and  $c$  can be deduced by fitting the the estimated exponents  $t(q)$  against the order  $q$  [45] In Fig. 6 the estimated values of the exponent  $t$  are shown as a function of  $q$  for the prime knots  $3_1$  and  $4_1$ . As usual in this kind of analysis [44], the plots of  $t(q)$  show deviations from linearity at relatively low  $q$ , due to finite  $N$  scaling correction effects. However, an optimal window of linearity can in general be identified for values of  $q$  which are somewhat larger, but not so large to cause problems with the sampling of the corresponding moments due to poor statistics. It makes sense then to rely to extrapolations

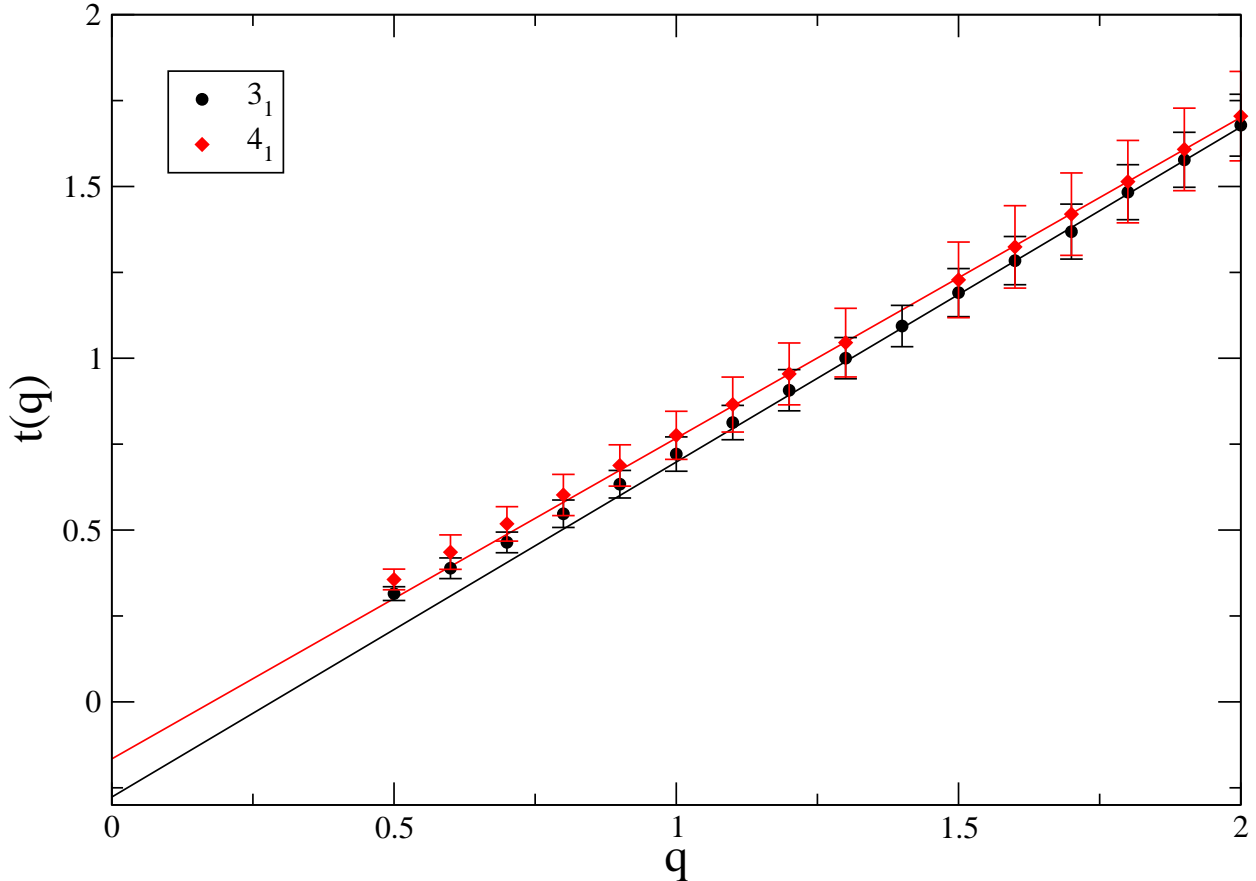


FIG. 6: Values of the exponents  $t(q)$  as a function of the order  $q$  of the moment for the knots  $3_1$  and  $4_1$ . The lines are best fits for  $1.3 < q < 2$ . There are deviations from the linear dependence for smaller values of  $q$  due to finite size effects.

of the linear behavior within these windows for a determination of both  $D$  and  $c$ . Indeed, from the slope and the intercept of these straight fitting lines we obtain the estimates given in table II for a number of different prime knots.

For  $3_1$  and  $4_1$  the estimates have been obtained by adding to the BFACF data those obtained with the pivot algorithm. We notice that  $D$  is reasonably close to the value we expected ( $D = 1$ ) especially for the  $3_1$  case. The discrepancy between the expected value and the measured one gets larger as the difficulty of sampling at large enough  $N$  increases. This sampling gets poorer with increasing knot complexity. Indeed the most reliable estimate of  $D$  is that obtained for the trefoil knot, for which the sampling is the best. Assuming for this knot  $D = 1$  and  $c = 1.25$  we would obtain  $t = 0.75$ . The estimates are all consistent with the expectation that prime knots are weakly localized in polymer rings in the swollen phase

<b>knot type</b>	<b>D</b>	<b>c</b>	<b>t</b>
3 <sub>1</sub>	0.958 ± 0.004	1.25 ± 0.04	0.72 ± 0.03
4 <sub>1</sub>	0.934 ± 0.004	1.18 ± 0.04	0.77 ± 0.04
5 <sub>1</sub>	0.918 ± 0.002	1.14 ± 0.03	0.79 ± 0.03
5 <sub>2</sub>	0.863 ± 0.003	1.11 ± 0.04	0.76 ± 0.04
7 <sub>1</sub>	0.864 ± 0.004	1.06 ± 0.09	0.81 ± 0.09

TABLE II: Results from the analysis of moments of the knot size PDF for the cut and join approach.

[14]. Moreover, compared with the estimates of Table I, those of table II vary considerably less with knot type. The results suggest that the knot length growth exponent  $t = t(1)$  for prime knots could be independent on the knot type.

## V. KNOT LENGTH ESTIMATES BY ENTROPIC COMPETITION

As remarked in the previous section, measures of the knot length based on the cut and join procedure lead to systematic errors that are somehow uncontrolled. These errors are mainly due to the topological interference between the chosen arc and the polygonal used to join the ends of the arc at infinity (Fig.4). This problem becomes much more serious in the case of collapsed ring polymers since the chance to find the ends of the arc deep inside the globule formed by the arc itself is very high. To overcome this problem, a completely different procedure has been recently introduced in Ref. [14]. The idea consists in partitioning a SAP into two (mutually avoiding) loops by a narrow slip-link that does not allow a complete migration of one loop, or of its knot, into the other loop. The whole topology of such structure can be characterized by the knot types  $\tau_1$  and  $\tau_2$ , respectively of the first and the second loop, and by the linking state between the two loops. On this model a Monte Carlo dynamics, based again on the BFACF algorithm, is then implemented in such a way that the overall topology of the configuration is conserved. In our simulations we considered only cases in which the two loops are unlinked. Let us start considering the most symmetric situation:  $\tau_1 = \tau_2$ . At equilibrium, since the number of configurations for the whole SAP is maximum when one of the loops is much longer than the other one, most configurations break the symmetry between the two loops showing a marked length unbalance. Typically,

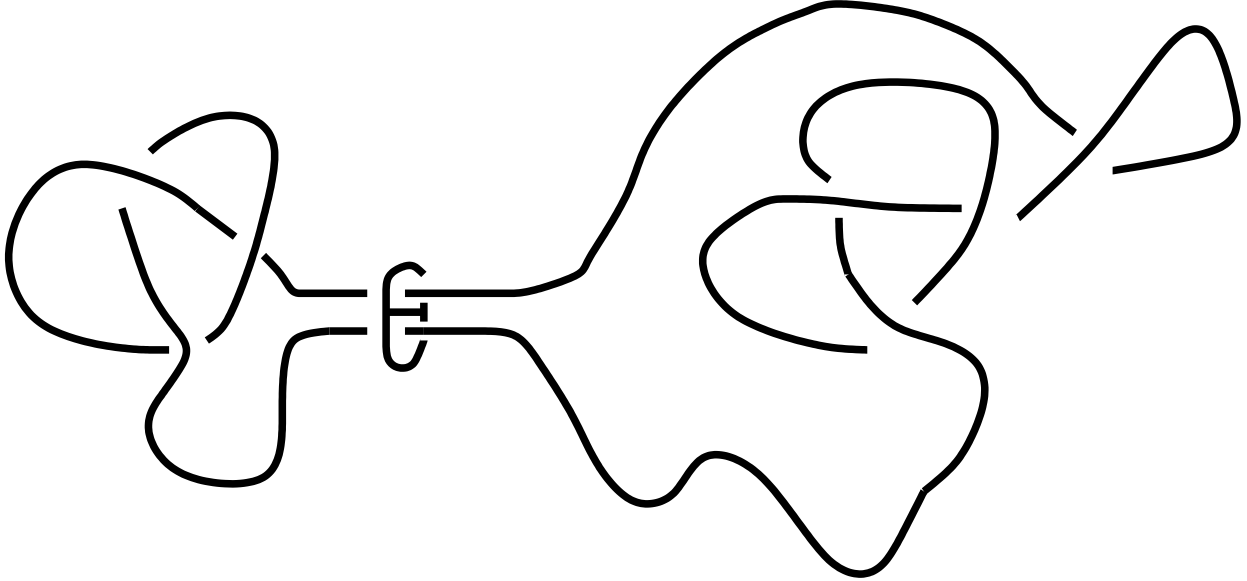


FIG. 7: Schetch of a trefoil knot forced to its typical length by the competition of another knot

in one of the two loops the knot has a very large share of the whole SAP at its disposal, while the other loop is just long enough to host its knot. This effect is very pronounced if both loops are unknotted ( $\tau_1 = \tau_2 = \emptyset$ ). In this case the smaller loop is practically always confined to the minimal length allowed by the model (Fig. 8). A similar behavior has been also found [42] for a model of independent loops, i.e. loops for which the mutual avoidance is neglected.

Consider now the situation in which each loop hosts the same prime knot ( $\tau_1 = \tau_2 \equiv \tau \neq \emptyset$ ). Here we identify the knot size  $\ell$  with the length of the smaller loop. With a little abuse of notation we are not going to distinguish between the length of the knot and the length of the shorter loop, as we will eventually argue that their scaling behaviors are the same. So, we will refer to both of them with the symbol  $\ell$ . Figure 9 shows the mean value of  $\ell$  as a function of the total size  $N$  for the cases  $\tau = 3_1, 4_1, 5_1$  and  $7_1$ . Unlike in the unknotted case, the size  $\ell$  is not fixed to the minimum value allowed by the knot type considered (for example 23 for  $3_1$  [46]), but fluctuates and grows according to

$$\langle \ell \rangle \sim N^t. \quad (3)$$

A log-log fit of the data gives for  $t$  estimates that are in agreement with those obtained by the direct measure of the knot length  $\ell$  based on the cut and join method. This corroborates the preliminary results in Ref. [14]. The analysis also confirms that the entropic competition

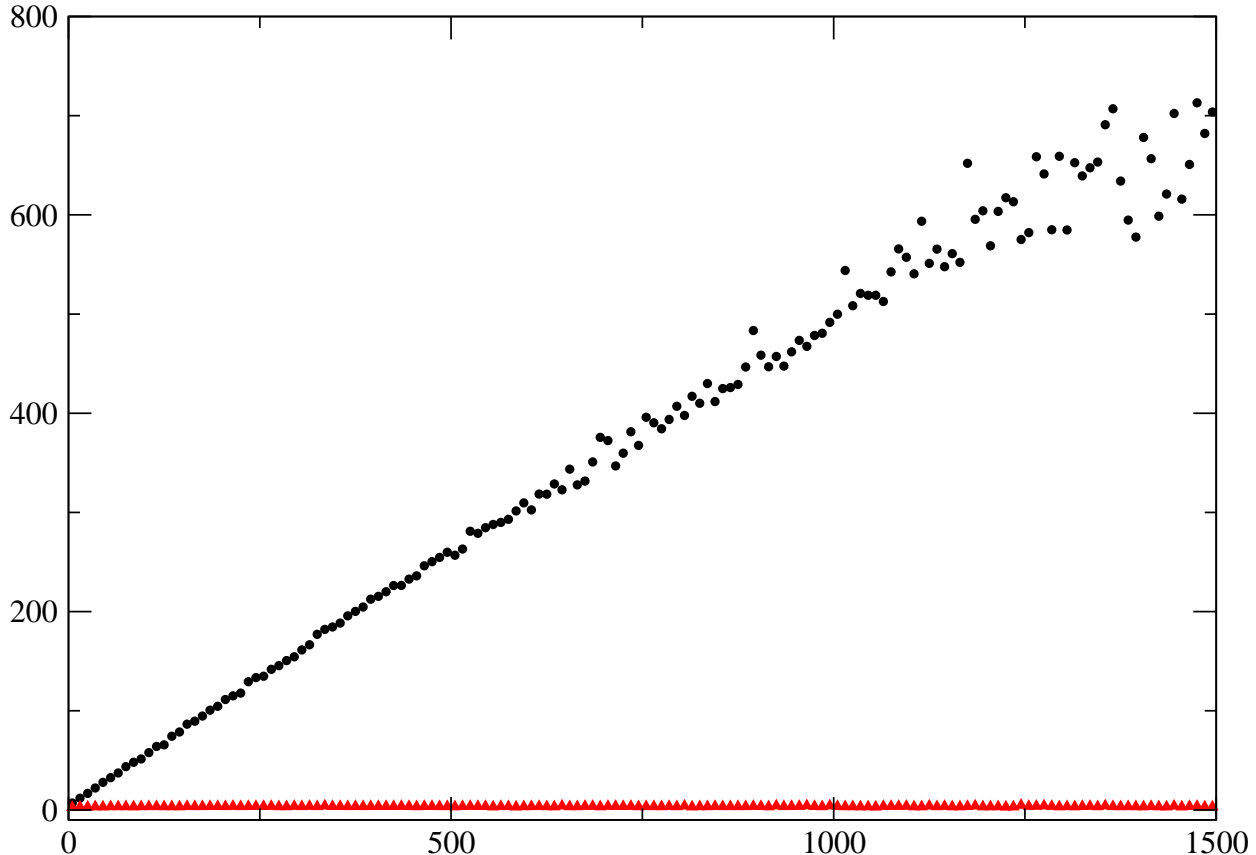


FIG. 8: Competition between unknotted loops: the circles represent the length of the longer loop while the triangles the length of the shorter loop. While the former delocalizes, the latter seems to be forced to its minimal length (4 edges).

approach is a valuable, alternative, tool for estimating the scaling behavior of the knot size. Note that, unlike the cut and join approach, the entropic competition method allows to estimate also the average size of composite knots when they are tightened close to each other within a tight loop. In Fig. 9, for example, we report the result for the case  $(3_1 \# 3_1, 3_1 \# 3_1)$ . It is interesting to notice that for this and other composite knots the  $N$  dependence of  $\langle \ell \rangle$  is similar to that observed for the prime knots considered. Thus, when the components of a composite knot are maximally localized, the exponent  $t$  does not seem to differ much from that valid for prime knot localization.

Why does the entropic competition method work so well? We learned from the cut and join approach that a knot hosted in a loop is weakly localized, i.e. its length grows as a power law of  $N$  with exponent  $t < 1$ . This means that the loop configuration in which the knot has strictly its minimal length (independent on  $N$ ) is not the only one favoured

entropically. In a system of two equally knotted loops one of the loops will always grow as  $N$  for the same entropic reasons we discussed in the case of two unknotted loops. Now, however, the smaller loop is knotted and since the knot tends to be weakly localized, it forces the whole loop to behave in the same way. Since the two loops host the same knot type, the situation is perfectly symmetric and the system chooses spontaneously which of the two loops to make longer. If, on the other hand, we break explicitly the loop symmetry by inserting different knots in the two loops, ( $\tau_1 \neq \tau_2$ ), the system at equilibrium tends to have as the smaller loop the one hosting the simpler of the two knots. The entropic argument described above for the smaller loop is still valid here and we do not expect changes in the scaling behavior of  $\langle \ell \rangle$ . This is indeed the case as one can see from Fig. 10, which shows the  $N$  dependence of  $\langle \ell \rangle$  in the cases in which the simplest knot is the trefoil ( $\tau_1 = 3_1$ ). In this case the average of  $\ell$  reported has been based on sampling the length of the loop with knot  $3_1$  only in configuration in which the same loop is the smaller one. One can notice that, as the complexity of  $\tau_2$  increases, the minimal length  $\ell_{min}$  to host such knot increases and, for fixed  $N$ , there would be less edges at disposal of the knot  $3_1$ . In other words the increase of the knot complexity in the longer loop corresponds to an increase of the “entropic force” it applies on the smaller loop. This action, however, affects only the amplitude of the scaling behavior of  $\langle \ell \rangle$ , keeping the exponent  $t$  unaltered as one can guess from the slopes of the log-log plots in Fig. 9.

As in the case of the direct measure, robust estimates of  $t$  can be obtained by performing the analysis of the moments if the probability distribution function  $p(\ell, N)$ , where  $\ell$  is the length of the shorter loop in the case of competition between two equal prime knots, or the length of the loop hosting the simpler knot (when it is also the shorter) in the case of two different competing knots. The obtained estimates for the exponents of  $p$  are reported in Table III. As one can see, they are compatible with those presented in Table II, obtained from the cut and join method.

## VI. KNOT SIZE IN COLLAPSED POLYGONS

If in the SAP model we introduce an attractive interaction between non consecutive n.n. monomers, we mimic the effect of a bad solvent. In this case, upon lowering the temperature below  $T_\Theta$ , the SAP undergoes a collapse transition [28] from a swollen to a collapsed phase.

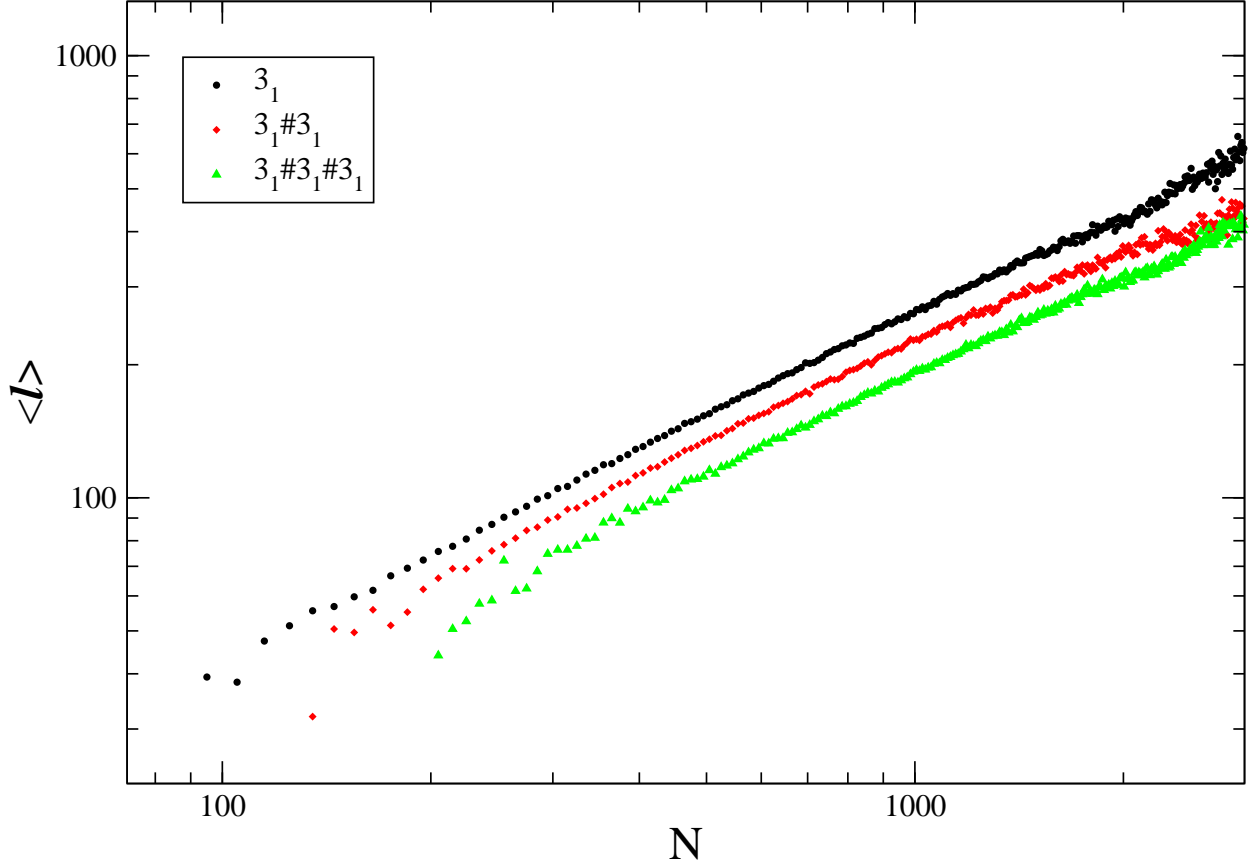


FIG. 9: Log-log plot of  $\langle \ell \rangle$  for the shorter loop as a function of  $N$ . Different symbols correspond to different knots  $\tau$  hosted by the second loop.

$(\tau_1, \tau_2)$	<b>D</b>	<b>c</b>	<b>t</b>
$3_1, 3_1$	$0.939 \pm 0.002$	$1.28 \pm 0.03$	$0.68 \pm 0.02$
$3_1\#3_1, 3_1$	$0.916 \pm 0.002$	$1.30 \pm 0.03$	$0.64 \pm 0.02$
$3_1\#3_1\#3_1, 3_1$	$0.940 \pm 0.005$	$1.33 \pm 0.04$	$0.63 \pm 0.03$
$4_1, 4_1$	$0.892 \pm 0.006$	$1.20 \pm 0.07$	$0.82 \pm 0.07$
$5_1, 5_1$	$0.939 \pm 0.002$	$1.14 \pm 0.05$	$0.81 \pm 0.04$
$7_1, 7_1$	$0.937 \pm 0.004$	$1.13 \pm 0.08$	$0.82 \pm 0.07$
$3_1\#3_1, 3_1\#3_1$	$0.940 \pm 0.002$	$1.07 \pm 0.06$	$0.87 \pm 0.06$

TABLE III: Estimates, with the method of moments, of the knot size exponent  $t$  obtained by looking at the average size of the smallest loop of the two loops model.

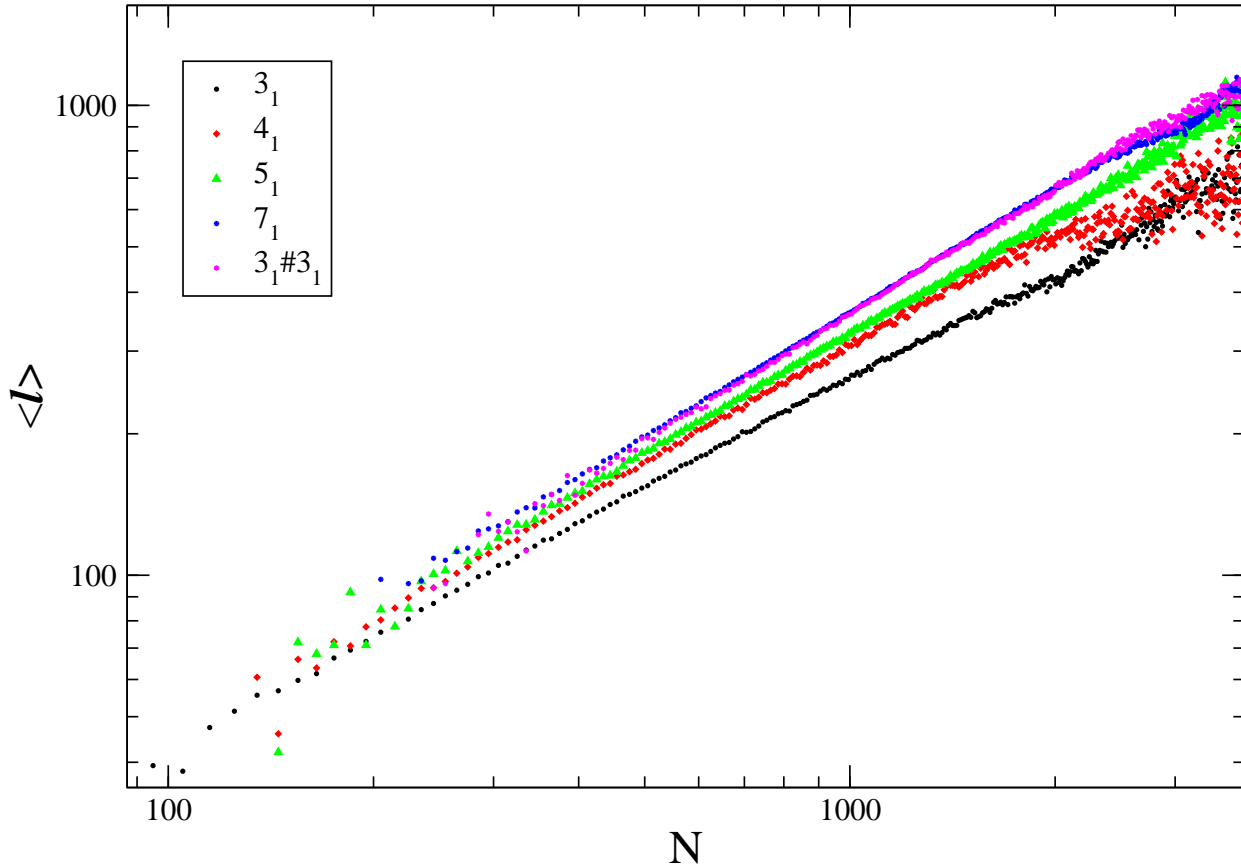


FIG. 10: Log-log plot of the mean length  $\langle \ell \rangle$  of the shortest loop (hosting  $3_1$ ) as a function of  $N$ . Different symbols correspond to different topologies of the longer loop.

It is interesting to see how the degree of localization of knots depends on the quality of the solvent. We are interested in determining how the size of the knot  $\ell$  behaves for highly condensed polygons. Previous studies on flat knots [25][27] showed that in the compact regime they delocalize. A similar delocalization was first predicted in Ref. [14] for real  $3d$  knots. Unfortunately an estimate of  $\langle \ell \rangle$  obtained by a cut and join method would not be reliable for compact configurations since the cut and close procedure would alter with high probability the topology of the chosen arc [48].

To the contrary, the strategy based on entropic competition does not involve alterations of the topology and should work also for very dense configurations. To obtain compact configurations we have simulated the two loop model at  $T \sim 0.53T_\Theta$ , i.e. well inside the collapsed phase. Unfortunately, to sample SAP's below the  $\Theta$  point is in general a difficult task to achieve [34]. The situation is even more delicate for grand canonical algorithms (such as the BFACF) since, at  $T < T_\theta$ , as the critical edge fugacity is approached from below, the

grand-canonical average number of SAP edges undergoes a first order infinite jump from a finite value, rather than growing continuously to infinity as in the  $T > T_\Theta$  case. In spite of this difficulty, we have been able to sample  $\sim 10^6$  uncorrelated configurations for each topology considered and for  $N$  up to  $\sim 700$ . In Fig. 11 the  $N$  dependence of  $\langle \ell \rangle$  is reported for the topologies  $(3_1, 3_1)$  and  $(4_1, 4_1)$ . For comparison the data coming from the swollen regime are also reported. The difference between the two regimes is evident and a linear behavior for the compact case can be easily guessed. Indeed, a simple linear fit of such data gives a good correlation coefficient ( $r = 0.9993$ ) and a slope  $A_{3_1} = 0.34$ .

An analysis of the moments of  $p(\ell, N)$  confirms the conclusion that the knots are delocalized in the globular phase. Indeed, e.g. in the case of the  $3_1$  knot, we obtain  $D \simeq 0.98$  and  $c \simeq 1.1$ , from plots of  $t(q)$  (Fig. 12) and this shows that the growth of the smaller loop is linear in the total length. A similar analysis for the figure eight case gives  $D \simeq 0.98$  and  $c \simeq 1.1$ , again consistent with the expected delocalization ( $t \simeq 1$ ).

## VII. THE MEAN RADIUS OF POLYGONS WITH FIXED KNOT TYPE: CORRECTION TO SCALING.

In this section we show how the weak localization property of knots in the swollen regime can have relevant consequences for the scaling behavior of the mean squared radius of gyration of SAP's with fixed knot type. According to the modern theory of critical phenomena based on the renormalization group (RG), its averaged large  $N$  behavior for a ring polymer is expected to be

$$\langle R_g^2 \rangle_N \sim AN^{2\nu} (1 + BN^{-\Delta} + o(N^{-\Delta})) \quad (4)$$

where the exponents  $\nu$  and  $\Delta$  are expected to be universal in the good solvent regime. They have been estimated as  $\nu = 0.5882 \pm 0.0010$  and  $\Delta = 0.478 \pm 0.010$  using field theoretic RG techniques ([49], see also [50]), consistent with the best available numerical estimates for lattice self-avoiding walks as given by Li *et al.* [51]:  $\nu = 0.5877 \pm 0.0006$ ,  $\Delta = 0.56 \pm 0.09$ .

These results are valid for phantom ring polymers with unrestricted topology, which are the only ones that can be treated on the basis of field theoretical RG methods. For a ring polymer with a fixed prime knot  $\tau$ , it is reasonable to expect an asymptotic form of  $\langle R_g^2 \rangle_{\tau, N}^{1/2}$  like that in Eq. (4), but possibly with different,  $\tau$ -dependent amplitudes. Since the  $\nu$  exponent is determined by the fractal structure of the polymer conformations, we do not

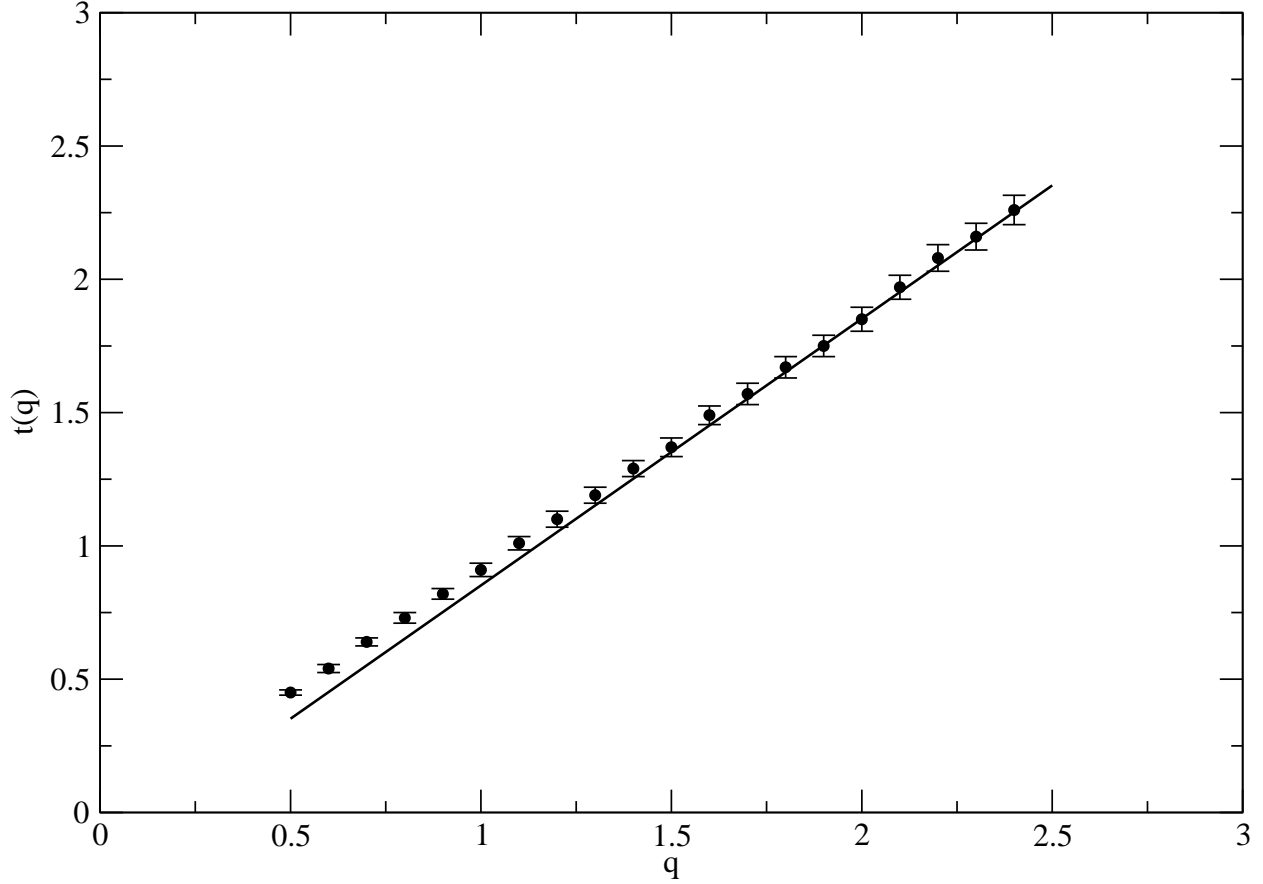


FIG. 11: Exponent  $t(q)$  in the competition between two trefoils in the compact phase. The data for the figure eight knots overlap those for trefoils, and are not included.

expect it to change as a consequence of a global restriction to a specific knot topology. To the contrary, for  $\Delta$  we expect the possibility of a deviation from the value reported in Eq. (5). Indeed, for the case of prime knots, we have established above a weak localization in the good solvent regime. This weak localization implies the existence of a characteristic length,  $\langle \ell \rangle^\nu \sim N^{t\nu}$ , diverging with a power of  $N$  which is subleading with respect to  $N^\nu$  ( $t < 1$ ). This gives the possibility of a scaling correction exponent  $\Delta' = 1 - t$ , as we argue below.

Let us write

$$\langle R_g^2 \rangle_{\tau, N} = A_\tau N^{2\nu} [1 + B_\tau N^{-\Delta_\tau} + o(N^{-\Delta_\tau})]. \quad (5)$$

for the asymptotic behavior of the mean square radius of gyration of a ring with fixed prime knot,  $\tau$ , in the swollen regime. In this expression we allow for a dependence of  $A$ ,  $B$  and  $\Delta$  on the type of knot. However, as far as  $A$  is concerned, we checked that the dependence on  $\tau$  is very weak.

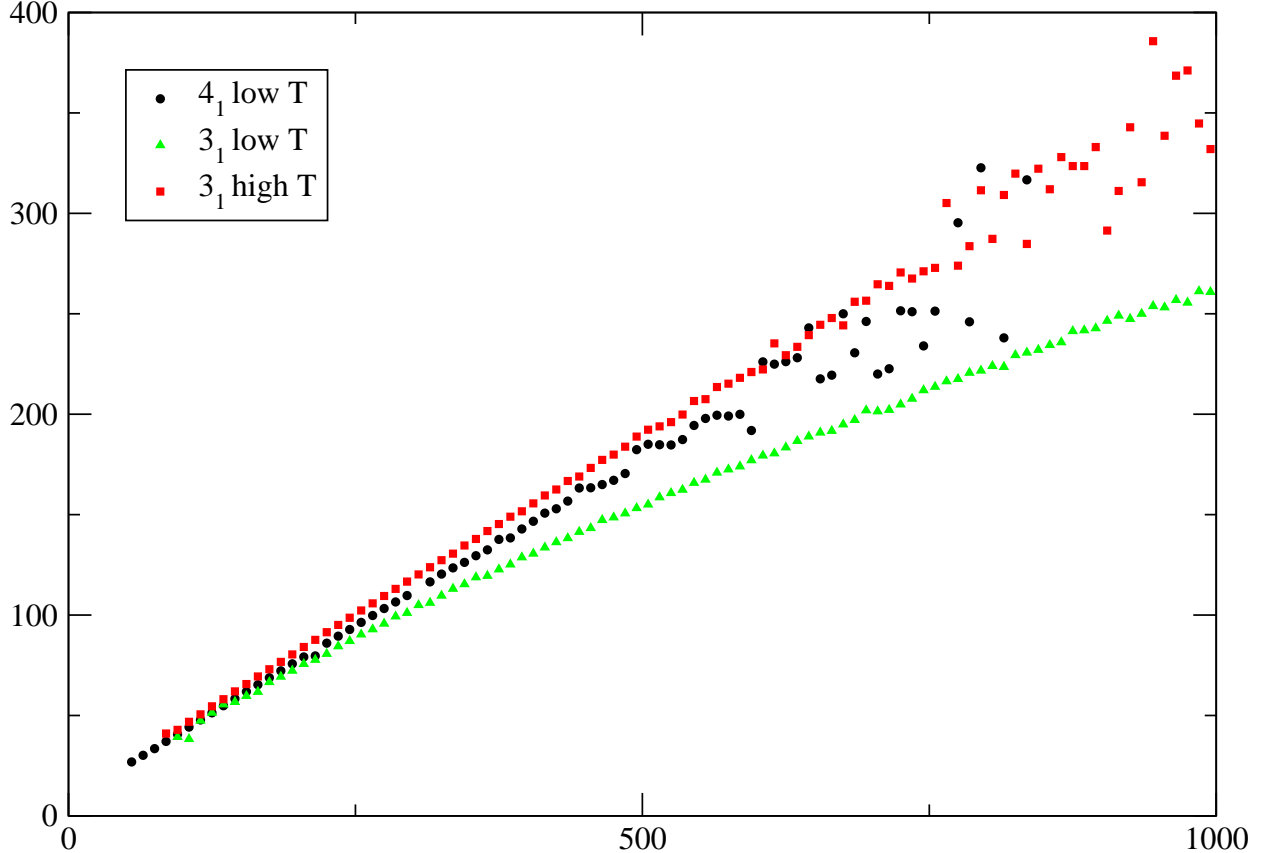


FIG. 12:  $N$  dependence of the average size of the shortest loop,  $\langle \ell \rangle$ , for the two loops model. The top curves corresponds respectively to the  $(4_1, 4_1)$  (Circles) and to the  $(3_1, 3_1)$  (Squares) topologies for  $T < T_\Theta$ . The bottom curve has been introduced for comparison and corresponds to the case  $T \gg T_\Theta$  for the topology  $(3_1, 3_1)$ .

For SAP's with fixed knot type  $\tau$ , let  $\langle \ell \rangle_\tau$  indicate the average size of the hosted knots. In general, if  $\langle \ell \rangle_\tau = o(N)$ , as  $N \rightarrow \infty$ ,  $\langle R_g^2 \rangle_{\tau, N}$  should scale as the size of an unknotted loop with length  $N - \langle \ell \rangle_\tau$ , i.e.

$$\langle R_g^2 \rangle_{\tau, N} \sim \langle R_g^2 \rangle_{\emptyset, N - \langle \ell \rangle_\tau} \quad (6)$$

Our estimates of  $\langle \ell \rangle_\tau$  suggest  $\langle \ell \rangle_\tau \sim a_\tau N^t$  with  $t \sim 0.75$ , roughly  $\tau$ -independent. By plugging this behavior in Eqs. (5) and (6) we obtain

$$\langle R_g^2 \rangle_{\tau, N} = A_\emptyset N^{2\nu} [1 + B_\emptyset N^{-\Delta_\emptyset} - C_\tau N^{t-1} + \dots] \quad (7)$$

where  $C_\tau = \nu a_\tau$ .

Eq. (7) implies that either  $\Delta_\emptyset$ , or  $(t-1)$  is the exponent describing the scaling correction

for a ring with fixed prime knot type  $\tau$ , independent of  $\tau$ . Below we indicate by  $\Delta'$  this correction exponent, and it will turn out  $\Delta' = 1 - t$  or  $\Delta' = \Delta_\emptyset$ , if  $1 - t < \Delta_\emptyset$  or  $\Delta_\emptyset < 1 - t$ , respectively. In any case, the fact that  $1 - t \sim 0.25$  tells us that  $\Delta'$  can not coincide with  $\Delta \sim 0.5$  of the phantom polymer.

Below we provide evidence that indeed  $\Delta' = 1 - t \simeq 0.25$  is quite plausible. At the same time one should conclude that, either  $B_\emptyset = 0$ , or  $\Delta_\emptyset > 1 - t$ .

In Ref. [13], the issue of the scaling of  $\langle R_g^2 \rangle_\tau$  was addressed without introducing the concept that knot localization could introduce a scaling correction exponent. A huge collection of data was analyzed by assuming also for the restricted knot topology the same correction exponent  $\Delta \sim 0.5$  predicted for the unrestricted case. In this way a rather convincing confirmation of the independence of  $\nu$  and  $A$  of  $\tau$  was obtained. To test the presence of a correction exponent  $(1 - t)$  we have replotted the data of Ref. [13], for  $\langle R_g^2 \rangle_\tau / N^{2\nu}$  assuming the scaling form (7) (see Figure VII) with a leading correction  $\sim N^{-\Delta'}$  and with  $\nu \simeq 0.588$ . Assuming a  $\Delta' \sim 1 - t < 0.5$ , the curves appear now more straight, as they should asymptotically, and extrapolate more clearly to a unique intercept with the ordinate axis, which estimates the common,  $\tau$ -independent, amplitude in Eq. (7). The fact that for the unknot the plot is almost horizontal suggest that either  $B_\emptyset = 0$ , or  $\Delta_\emptyset$  is sensibly larger than  $1 - t$ . This becomes more clear if one plots, on the same figure, the  $N$  dependence of  $\langle R_g^2 \rangle_{3_1, N} / N^{2\nu}$  by using different correction terms. As one can see the data rescaled with  $\Delta' = 1 - t \sim 0.25$  are clearly more on a straight line than those rescaled with  $\Delta = 0.5$  or with a much stronger, hypothetical, correction  $\Delta = 0.1$ .

In table IV are reported the estimates of the amplitudes  $A_\emptyset$  corresponding to the unknot, and to the  $3_1$  and  $4_1$  knots, extrapolated from plots like those in Fig. 14, in the cases  $\Delta' = 0.10$ ,  $\Delta' = 0.25$ , and  $\Delta' = 0.5$ . The fact that for  $\Delta' = 0.25$  there is an optimal agreement among the three values further supports our conclusions on  $\Delta'$ .

## VIII. DISCUSSION

In this work we addressed the problem of localization of knots in flexible ring polymers modelled by SAPs on cubic lattice.

In the swollen regime we showed that a statistical method of prime knot length determination based on isolating different portions of the SAP as candidates to host the knot

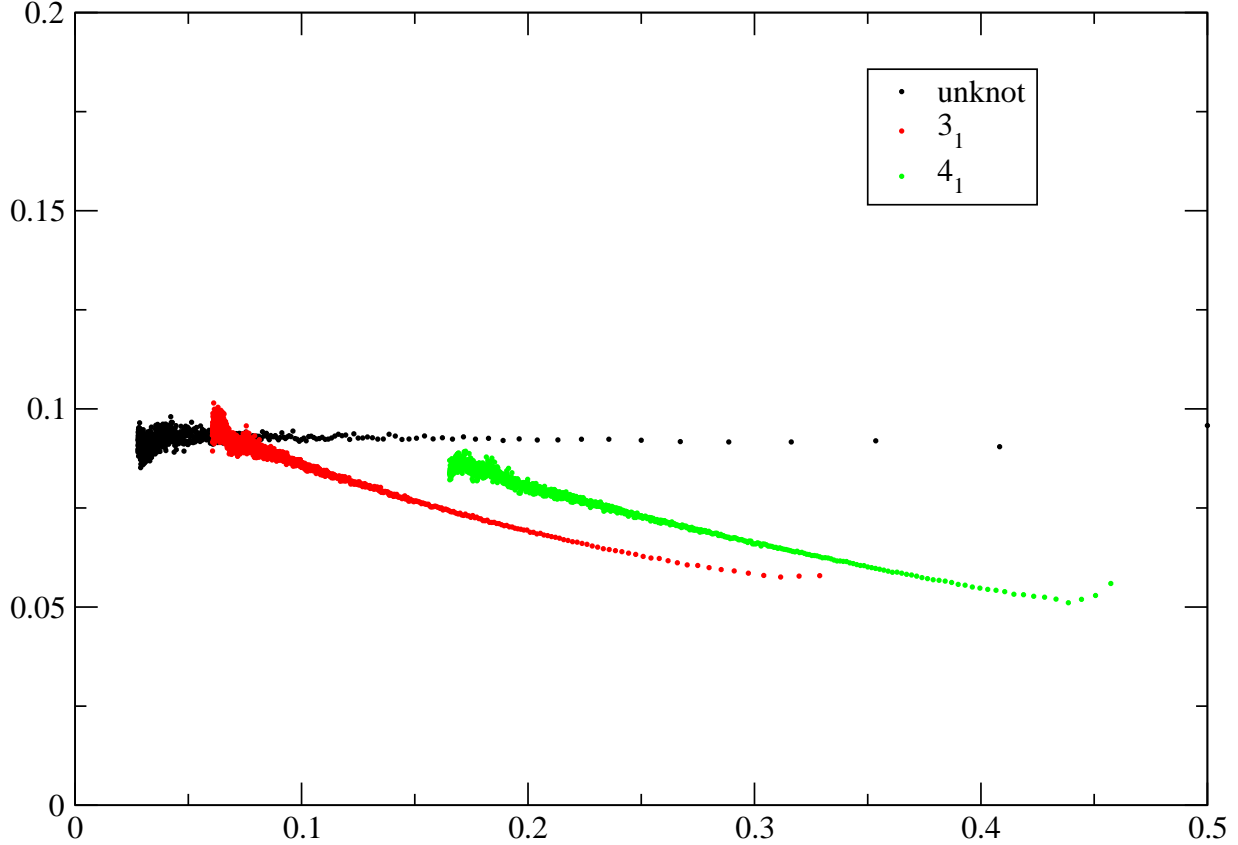


FIG. 13: Plot of  $R_g^2/N^{2\nu}$  against  $N^{-\Delta'}$  for the unknot ( $\emptyset$ ),  $3_1$  and  $4_1$ .  $\Delta' = 0.25$  is considered.

$\Delta$	unknot	$3_1$	$4_1$
0.1	$0.101 \pm 0.004$	$0.172 \pm 0.004$	$0.152 \pm 0.003$
$1 - t$	$0.102 \pm 0.004$	$0.110 \pm 0.004$	$0.112 \pm 0.004$
0.5	$0.102 \pm 0.004$	$0.108 \pm 0.005$	$0.095 \pm 0.005$

TABLE IV: Estimates of the amplitude  $A(\emptyset)$  in eq. 4 for different knot type and with  $\nu(\emptyset) = 0.588$ . Different estimates correspond to different value of the correction to scaling exponent  $\Delta$ . For the unknot the values  $\Delta = 1 - t$  and  $\Delta = 0.5$  coincide.

is consistent with an alternative criterion, based on the entropic competition between two knotted loops within the same ring. By a systematic analysis of the moments of the knot length PDF of different knots, we gave strong indication that the localization of a prime knot is characterized by an exponent  $t \sim 0.75$  describing how the average length grows as

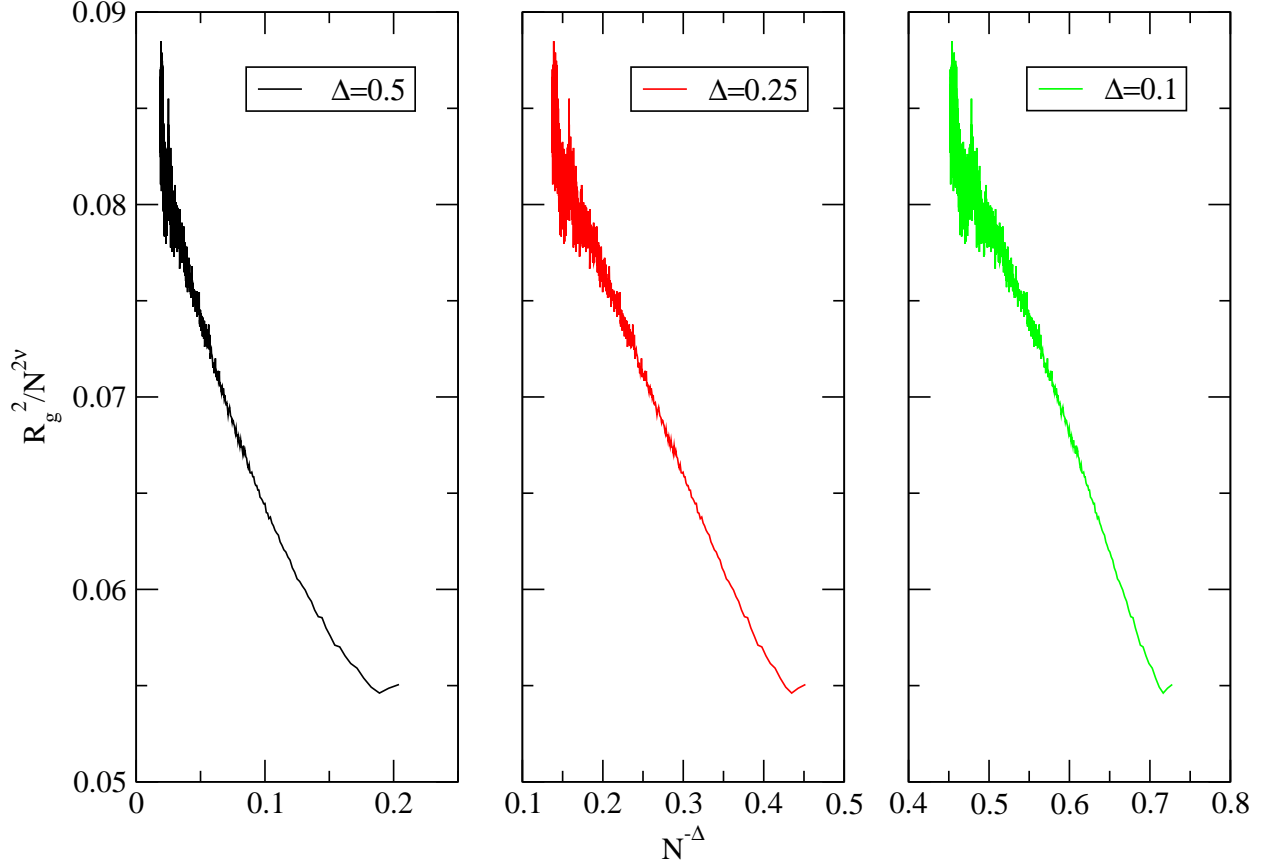


FIG. 14: Plot of  $R_g^2/N^{2\nu}$  versus  $N^{-\Delta}$  for three different values of  $\Delta$  for  $3_1$ . From left to right: the standard value for  $\Delta$  used for ensembles with unrestricted topology ( $\Delta = 0.5$ ), the correction coming from our data for polymers with a prime knot in it ( $\Delta = 0.28$ ), and then a greater correction ( $\Delta = 0.1$ ). As one can notice, the best correction seems to be given by the intermediate value between the three proposed. These data are the ones proposed in Figure 7 of Ref.[13].

a function of  $N$ . The exponent  $t$  could be universal for different prime knots, or even for composite knots whose components are tightened to remain close to each other in the same loop.

We have shown that the weak localization of a prime knot in a swollen ring determines a peculiar scaling correction exponent  $\Delta' = 1 - t \simeq 0.25$  for the asymptotic scaling of the radius of gyration. This exponent implies a stronger correction compared to that occurring for phantom ring polymers with unrestricted knot type. We think that recent works in the literature, addressing subtle issues concerning the scaling of polymer rings with fixed topology [52], could sharpen their conclusions by taking into account in the numerical analysis

the different scaling correction identified here.

A remarkable advantage of the method of entropic competition between knotted loops is the possibility of dealing with the collapsed regime without risking to suffer too strong systematic errors in the determination of the knot length. Thanks to a systematic analysis of data we could conclude that both prime and composite knots fully delocalize in the globular phase, confirming a previous prediction by the authors of the present work [14].

## **IX. AKNOLEDGMENT**

This work was supported by FIRB01 and MIUR-PRIN05.

- 
- [1] P.G. de Gennes, *Scaling Concepts in Polymer Physics*, (Cornell University Press, Ithaca, New York, 1979).
- [2] M. Doi and S.F. Edwards, *The theory of Polymer Dynamics*, (Clarendon Press, Oxford, 1986).
- [3] B. Alberts, K. Roberts, D. Bray, J. Lewis, M. Raff and J.D. Watson, *The molecular biology of the cell*, (Garland, New York, 1994).
- [4] V.V. Rybenkov, N.R. Cozzarelli and A.V. Vologodskii, Proc. Natl. Acad. Sci. USA **90**, 5307 (1993).
- [5] S. Y. Shaw and J.C. Wang, Science **260**, 533 (1993).
- [6] Pieransky P., Kasas S., Dietler G., Dubochet J. and Stasiak A. New J. Phys. **3**, 10 (2001).
- [7] W. T. Taylor, Nature **392**, 916 (2000).
- [8] Lua R. C., Grosberg A. Y., Plos Comput Biol, **2**(5) e45, (2006).
- [9] Virnau P., Mirny L. A., Kardar M., Plos Computational Biology, **2**(9), e122 (2006).
- [10] B. Marcone, E. Orlandini, A. L. Stella and F. Zonta, *Knots in proteins*, in preparation.
- [11] D.W. Sumners and S.G. Whittington, J. Phys. A: Math. Gen. **21**, 1689 (1988).
- [12] Pippenger N., Disc. Appl. Math. **25**, 273 (1989).
- [13] E. Orlandini, M.C. Tesi, E.J. Janse van Rensburg and S.G. Whittington, J. Phys. A: Math. Gen. **31**, 5953-5967 (1998).
- [14] B. Marcone, E. Orlandini, A.L. Stella and F. Zonta, J. Phys. A: Math. Gen. L1-L7 (2004).
- [15] A. Stasiak, V. Katrich, J. Bednar, D. Michout and J. Dubochet, Nature **384**, 122 (1996).
- [16] Y. Arai, R. Yasuda, K. Akashi, Y. Harada, H. Miyata, K. Kinoshita and H. Itoh, Nature, **399**, 446 (1999).
- [17] X.R. Bao, H.J. Lee and S.R. Quake Phys. Rev. Lett. **91**, 265506 (2003).
- [18] V. Katrich, W. K. Olson, A. Vologodskii, J. Dubochet and A. Stasiak, Phys. Rev. E **61**, 5545 (2000).
- [19] E.J. Janse van Rensburg, D.A.W. Sumners, E. Wasserman and S.G. Whittington, J. Phys. A: Math. Gen. **25**, 6557 (1992).
- [20] D. Rolfsen, *Knots and Links*, (Berkely, CA: Publish or Perish)(1990).
- [21] E. Gutter and E. Orlandini, J. Phys. A: Math. Gen. **32**, 1359 (1999).
- [22] R. Metzler, A. Hanke, P. G. Dommersnes, Y. Kantor and M. Kardar, Phys. Rev. Lett. **88**,

- 188101 (2002).
- [23] B. Maier and J. O. Rädler, Phys. Rev. Lett. **82**, 1911 (1999).
- [24] E. Ben-Naim, Z.A. Daya, P. Vorobieff and R.E. Ecke, Phys. Rev. Lett. **86**, 1414 (2001).
- [25] E. Orlandini, A.L. Stella And C. Vanderzande, Phys. Rev. E **68**, 031804 (2003).
- [26] E. Orlandini, A.L. Stella And C. Vanderzande, J. Stat. Phys, **115**, 681 (2004).
- [27] A. Hanke, R. Metzler, P.G. Dommersnes, Y. Kantor and M. Kardar, Euro. Phys. J. E **12**, 347 (2003).
- [28] C. Vanderzande, *Lattice models of Polymers*, Cambridge University Press, Cambridge (1998).
- [29] P. Virnau, Y. Kantor, and M. Kardar, J. of Am. Chem. Soc. **127**, 43 (2005).
- [30] O. Farago, Y. Kantor, M. Kardar, Europhys. Lett. **60**, 53 (2002).
- [31] S. Caracciolo, A. Pellissetto and A.D. Sokal, J. Stat. Phys **60**, 1 (1990).
- [32] A. D. Sokal, hep-lat/9405016 in *Monte Carlo and Molecular Dynamics Simulation in Polymer Science*, ed. K. Binder (Oxford University Press, New York 1995).
- [33] E.J. Janse van Rensburg and S.G. Whittington, J. Phys. A.: Math. Gen. **24**, 5553 (1991).
- [34] M.C. Tesi, E.J. Janse van Rensburg, E. Orlandini and S.G. Whittington, J. Stat. Phys. **29**, 2451 (1996).
- [35] E. Orlandini, *Numerical methods for Polymeric Systems (IMA Volumes in Mathematical and its Applications)*, vol. 102, ed. S Whittington (Berlin: Springer).
- [36] Note that the critical value of  $K_c$  for 3D self-avoiding walks has been estimated to be 0.213496 (see A.J. Guttmann J. Phys. A **22**, 2807 (1989)).
- [37] N. Madras and G. Slade, *The self avoiding walk*, Birkhäuser (1993). N. Madras, A. Orlitsky and L. Shepp. J. Stat. Phys. **58**, 159 (1990).
- [38] A. Yao, H. Marsuda, H. Tsukahara, M.K. Shimamura and T Deguchi, J. Phys. A **34**, 7563 (2001).
- [39] Y. Kantor and M. Kardar, ARI The Bulletin of the Istanbul Technical University **54**, 1, (2004).
- [40] K. Millet, A. Dobay and A. Stasiak, Macromolecules **38**, 601-606, (2005).
- [41] A. V. Vologodskii, A.V. Lukashin, H.D. Frank-Kamenetskii, and V.V. Anshelevich, Sov. Phys. J.E.T.P **66**, 2153 (1974).
- [42] R. Zandi, Y. Kantor and M. Kardhar, ARI The bulletin of the ITU, **53** 6 (2003).
- [43] E. Carlon, E. Orlandini and A.L. Stella, Phys. Rev. Lett. **88** , 198101 (2002).
- [44] C. Tebaldi, M. De Menech and A.L. Stella, Phys. Rev. Lett. **83**, 3952 (1999).

- [45] Since for the distribution in Eq. (1) it is found in general that  $t(q) = 0$  for  $q \leq q_c$  with  $q_c > 0$ , the normalization constraint  $\int p(\ell, N) = 1$  does not imply  $D(1 - c) = 0$  i. e.  $c = 1$ .
- [46] Y. Diao, J. Stat. Phys. **74**, 1247 (1994).
- [47] K. Koniaris, M. Muthukumar, Phys. Rev. Lett. **66**, 2211-2214 (1991). K. Koniaris, M. Muthukumar, J. Chem. Phys. **95**, 2873-2881 (1991).
- [48] In spite of this, recent study in Ref. [29] of an off lattice model of polyethylene chains addressed the issue of localization for the  $3_1$  knot in the collapsed phase and gave result supporting those of Ref. [14] for SAPs. These authors used methods previously proposed by Koniaris and Muthukumar [47] and by Taylor [7] for the detection and the localization of knots in open chains.
- [49] R. Guida and J. Zinn-Justin, J. Phys. A: Math. and Gen. **31**, 8103 (1998).
- [50] J.C. Le Guillou and J. Zinn-Justin, Phys. Rev. B **21**, 3976 (1980). J.C. Le Guillou and J. Zinn-Justin, J. Physique **50**, 1365 (1989).
- [51] Li B., Madras N. and Sokal A. D., J. Stat. Phys., **80**, 661 (1995).
- [52] A. Dobay, J. Dubochet, K. Millett, P.E. Sottas and A. Stasiak, PNAS **10**, 5611 (2003).